

A Domain-adaptive Physics-informed Neural Network for Inverse Problems of Maxwell's Equations in Heterogeneous Media

Shiyuan Piao, Hong Gu, Aina Wang, Pan Qin

Abstract—Maxwell's equations are a collection of coupled partial differential equations (PDEs) that, together with the Lorentz force law, constitute the basis of classical electromagnetism and electric circuits. Effectively solving Maxwell's equations is crucial in various fields, like electromagnetic scattering and antenna design optimization. Physics-informed neural networks (PINNs) have shown powerful ability in solving PDEs. However, PINNs still struggle to solve Maxwell's equations in heterogeneous media. To this end, we propose a domain-adaptive PINN (da-PINN) to solve inverse problems of Maxwell's equations in heterogeneous media. First, we propose a location parameter of media interface to decompose the whole domain into several sub-domains. Furthermore, the electromagnetic interface conditions are incorporated into a loss function to improve the prediction performance near the interface. Then, we propose a domain-adaptive training strategy for da-PINN. Finally, the effectiveness of da-PINN is verified with two case studies.

Index Terms—Domain-adaptive physics-informed neural network, domain-adaptive training strategy, Maxwell's equations in heterogeneous media.

I. INTRODUCTION

MAXWELL'S equations are used to describe the fundamental laws of electromagnetic fields [1], which are widely used in geological exploration [2], medical imaging [3], and many other fields [4], [5]. The Maxwell's equations are classically solved by numerical methods [6], such as finite-difference time-domain method [7], finite element method [8], Born iterative method [9], and variational Born iteration method [10]. However, one of the challenges these numerical methods face is the high computational cost [11].

The deep learning methods with remarkable approximation capability have attracted increasing attention in solving partial differential equations (PDEs) [12], [13]. The physics-informed neural networks (PINNs) proposed in [14] are prevalent mesh-free methods for solving PDEs. In the framework of PINNs, the prior knowledge of physics and sparse measurements are incorporated into the loss function to train PINNs. Successful achievements in estimating the parameters of PDEs with homogeneous media, such as supersonic flows [15], beam systems [16], and nano-optics [17], have been reported [18], [19]. Meanwhile, the Maxwell's equations in heterogeneous

media have wide applications, such as nondestructive testing of multilayered coating [20], [21]. However, it remains a challenge for PINNs to solve inverse problems in heterogeneous media composed of several homogeneous media [22]. In the heterogeneous media case, the parameters of PDEs are not fixed in the whole domain and will jump at media interface. Such parameter jumping can potentially lead to PINNs could not work well. In [23], [24], PINNs were used to solve inverse problems of the Maxwell's equations in heterogeneous media. However, these methods obtain inaccurate estimations near the interface due to the interface conditions not being considered, as indicated in our experiments.

To solve the aforementioned problems, this letter proposes a domain-adaptive PINN (da-PINN) for the Maxwell's equations in heterogeneous media. The goal of da-PINN is to estimate parameters of the Maxwell's equations and predict the electric and magnetic fields. We first propose a location parameter of media interface to decompose the whole domain into several sub-domains under the assumption of each sub-domain with fixed parameters of the Maxwell's equations. Then, sub-networks are constructed to approximate electric and magnetic fields in each sub-domain. The electromagnetic interface conditions are incorporated into a loss function. In addition, a domain-adaptive training strategy is proposed to optimize da-PINN. Finally, the performance of da-PINN is verified with one- and two- dimensional Maxwell's equations in heterogeneous media.

This letter is organized as follows. In Section II, we introduce PINNs for a derivative of vector-valued functions and da-PINN. In Section III, da-PINN is verified with one- and two- dimensional cases. Section IV concludes this letter.

II. METHODOLOGY

A. PINNs for Derivatives of Vector-valued Functions

In this section, we briefly introduce PINNs for inverse problems in the derivative of vector-valued functions, the general form is as follows:

$$\mathbf{u}_t(t, \mathbf{x}) + \mathcal{N}[\mathbf{u}(t, \mathbf{x}); \boldsymbol{\lambda}] = 0, \quad \mathbf{x} \in \Omega \subseteq \mathbb{R}^D, \quad t \in [0, T]. \quad (1)$$

Here, $\mathbf{u} : \mathbb{R} \times \mathbb{R}^p \rightarrow \mathbb{R}^q$ denotes the solution with spatiotemporal dependence, \mathbf{u}_t is the partial derivative of \mathbf{u} with respect to t , \mathcal{N} is a vector differential operator parameterized by an unknown real-valued vector $\boldsymbol{\lambda} \in \mathbb{R}^m$, (t, \mathbf{x}) is a pair-wised

coordinate of the time t and space \mathbf{x} . A residual function $\mathbf{f}(t, \mathbf{x})$ is defined as follows:

$$\mathbf{f} = \mathbf{u}_t + \mathcal{N}[\mathbf{u}; \boldsymbol{\lambda}]. \quad (2)$$

In PINNs, $\hat{\mathbf{u}}(t, \mathbf{x}; \boldsymbol{\theta})$ is a fully-connected neural network (FCNN) to approximate \mathbf{u} satisfying (1), in which $\boldsymbol{\theta}$ is a set of weights. PINNs can be trained using the following loss function:

$$Loss(\boldsymbol{\theta}, \boldsymbol{\lambda}) = Loss_D(\boldsymbol{\theta}) + Loss_P(\boldsymbol{\theta}, \boldsymbol{\lambda}), \quad (3)$$

where

$$Loss_D(\boldsymbol{\theta}) = \frac{1}{N} \sum_{(t, \mathbf{x}, \mathbf{u}) \in D_D} \|\hat{\mathbf{u}}(t, \mathbf{x}; \boldsymbol{\theta}) - \mathbf{u}\|_2^2$$

is a data-driven loss;

$$Loss_P(\boldsymbol{\theta}, \boldsymbol{\lambda}) = \frac{1}{N} \sum_{(t, \mathbf{x}) \in D_C} \|\hat{\mathbf{f}}(t, \mathbf{x}; \boldsymbol{\theta}, \boldsymbol{\lambda})\|_2^2$$

is a physics-informed loss; $D_D = \{(t_j, \mathbf{x}_j, \mathbf{u}_j) | j = 1, 2, \dots, N\}$ denotes the training dataset; $D_C = \{(t_j, \mathbf{x}_j) | j = 1, 2, \dots, N\}$ denotes the collocation point set. Unknown $\boldsymbol{\lambda}$ is treated as weights of neural networks and will be optimized by the gradient descent method. The automatic differentiation (AD) [25] is used to numerically calculate \mathbf{u}_t and $\mathcal{N}[\mathbf{u}; \boldsymbol{\lambda}]$.

B. da-PINN for Maxwell's Equations in Heterogeneous Media

The passive and lossless Maxwell's equations under study are of the following generalized form:

$$\begin{aligned} \nabla \times \mathbf{E}(t, \mathbf{x}) &= -\mu(\mathbf{x}) \frac{\partial \mathbf{H}(t, \mathbf{x})}{\partial t}, \\ \nabla \times \mathbf{H}(t, \mathbf{x}) &= \varepsilon(\mathbf{x}) \frac{\partial \mathbf{E}(t, \mathbf{x})}{\partial t}, \end{aligned} \quad (4)$$

with

$$\mu(\mathbf{x}) = \begin{cases} \mu_1, & \text{if } \mathbf{x} \in \Omega_1 \\ \mu_2, & \text{if } \mathbf{x} \in \Omega_2 \end{cases}, \quad \varepsilon(\mathbf{x}) = \begin{cases} \varepsilon_1, & \text{if } \mathbf{x} \in \Omega_1 \\ \varepsilon_2, & \text{if } \mathbf{x} \in \Omega_2 \end{cases}.$$

Here, \mathbf{E} is the electric field vector, \mathbf{H} is the magnetic field vector, μ is the magnetic permeability, ε is the electric permittivity, Ω is a spatial close set with heterogeneous media, which is composed of two homogeneous media. ∇ denotes the del operator, and \times denotes the cross product. Ω is divided into $\Omega_1 \cup \Omega_2$. The interface $\psi = \partial\Omega_1 \cap \partial\Omega_2$ with ∂ being the boundary.

According to [26], the electromagnetic interface conditions under study are as follows:

$$\begin{cases} E_{1t} = E_{2t}, & H_{1t} = H_{2t} \\ \varepsilon_1 E_{1n} = \varepsilon_2 E_{2n}, & \mu_1 H_{1n} = \mu_2 H_{2n} \end{cases},$$

where E_{it} and E_{in} are the tangential and normal components of electric fields in Ω_i , respectively. H_{it} and H_{in} are the tangential and normal components of magnetic fields in Ω_i , respectively. In this letter, $i = 1, 2$. Residual functions for the Maxwell's equations and interface conditions are defined as

follows:

$$\mathbf{f} = \nabla \times \mathbf{E} + \mu \frac{\partial \mathbf{H}}{\partial t}, \quad (5)$$

$$\mathbf{h} = \nabla \times \mathbf{H} - \varepsilon \frac{\partial \mathbf{E}}{\partial t}, \quad (6)$$

$$\begin{aligned} s &= (E_{1t} - E_{2t})^2 + (H_{1t} - H_{2t})^2 \\ &+ (\varepsilon_1 E_{1n} - \varepsilon_2 E_{2n})^2 + (\mu_1 H_{1n} - \mu_2 H_{2n})^2. \end{aligned} \quad (7)$$

Assume that ψ in Ω is perpendicular to the x -axis, but the exact location of ψ , i.e., $x = d$ is unknown. To this end, da-PINN is proposed to estimate the parameter vector $\boldsymbol{\lambda} = [\mu_1, \varepsilon_1, \mu_2, \varepsilon_2, d]^\top$ and predict \mathbf{E} and \mathbf{H} ; da-PINN can be trained using the following loss function:

$$Loss(\boldsymbol{\theta}_1, \boldsymbol{\theta}_2, \boldsymbol{\lambda}) = Loss_D(\boldsymbol{\theta}_1, \boldsymbol{\theta}_2) + Loss_P(\boldsymbol{\theta}_1, \boldsymbol{\theta}_2, \boldsymbol{\lambda}) + Loss_I(\boldsymbol{\theta}_1, \boldsymbol{\theta}_2, \boldsymbol{\lambda}), \quad (8)$$

where

$$\begin{aligned} Loss_D(\boldsymbol{\theta}_1, \boldsymbol{\theta}_2) &= \frac{1}{N_{D_1}} \sum_{(t, \mathbf{x}, \mathbf{u}) \in D_{D_1}} \|\hat{\mathbf{u}}_1(t, \mathbf{x}; \boldsymbol{\theta}_1) - \mathbf{u}\|_2^2 \\ &+ \frac{1}{N_{D_2}} \sum_{(t, \mathbf{x}, \mathbf{u}) \in D_{D_2}} \|\hat{\mathbf{u}}_2(t, \mathbf{x}; \boldsymbol{\theta}_2) - \mathbf{u}\|_2^2 \end{aligned}$$

is a data-driven loss;

$$\begin{aligned} Loss_P(\boldsymbol{\theta}_1, \boldsymbol{\theta}_2, \boldsymbol{\lambda}) &= \frac{1}{N_{P_1}} \sum_{(t, \mathbf{x}) \in C_{P_1}} \left\{ \|\hat{\mathbf{f}}_1(t, \mathbf{x}; \boldsymbol{\theta}_1, \boldsymbol{\lambda})\|_2^2 \right. \\ &+ \|\hat{\mathbf{h}}_1(t, \mathbf{x}; \boldsymbol{\theta}_1, \boldsymbol{\lambda})\|_2^2 \left. \right\} + \frac{1}{N_{P_2}} \sum_{(t, \mathbf{x}) \in C_{P_2}} \left\{ \|\hat{\mathbf{f}}_2(t, \mathbf{x}; \boldsymbol{\theta}_2, \boldsymbol{\lambda})\|_2^2 \right. \\ &+ \|\hat{\mathbf{h}}_2(t, \mathbf{x}; \boldsymbol{\theta}_2, \boldsymbol{\lambda})\|_2^2 \left. \right\} \end{aligned}$$

is a physics-informed loss;

$$Loss_I(\boldsymbol{\theta}_1, \boldsymbol{\theta}_2, \boldsymbol{\lambda}) = \frac{1}{N_I} \sum_{(t, \mathbf{x}) \in C_I} \hat{s}(t, \mathbf{x}; \boldsymbol{\theta}_1, \boldsymbol{\theta}_2, \boldsymbol{\lambda})^2$$

is an interface-condition loss; $\hat{\mathbf{u}}_i(t, \mathbf{x}; \boldsymbol{\theta}_i) = [\hat{\mathbf{E}}_i(t, \mathbf{x}; \boldsymbol{\theta}_i)^\top, \hat{\mathbf{H}}_i(t, \mathbf{x}; \boldsymbol{\theta}_i)^\top]^\top$ is the function of the constructed Net_i with $\boldsymbol{\theta}_i$ being a set of weights. $D_D = D_{D_1} \cup D_{D_2}$, $D_{D_i} = \{(t_j, \mathbf{x}_j, \mathbf{u}_j) | j = 1, 2, \dots, N_{D_i}\}$ and $C_{P_i} = \{(t_j, \mathbf{x}_j) | j = 1, 2, \dots, N_{P_i}\}$ are the training dataset and collocation point sets, respectively. They are randomly sampled from the whole domain. $C_I = \{(t_j, \mathbf{x}_j) | j = 1, 2, \dots, N_I\}$ is the collocation point set randomly sampled from the interface; $\hat{\mathbf{f}}_i, \hat{\mathbf{h}}_i$, and \hat{s} are obtained according to (5)-(7).

A domain-adaptive training strategy shown in Algorithm 1 is proposed to achieve $\boldsymbol{\theta}_i$ and $\boldsymbol{\lambda}$ simultaneously. Let k denote iterative step. In Algorithm 1, we take $\nu^{(k)} d^{(k)}$ as the x -axis coordinate of $C_{P_1}^{(k)}$, $\nu^{(k)} (B - d^{(k)}) + d^{(k)}$ as the x -axis coordinate of $C_{P_2}^{(k)}$, and $d^{(k)}$ as the x -axis coordinate of $C_I^{(k)}$. Here, $\nu^{(k)} \stackrel{i.i.d.}{\sim} U(0, 1)$ and $x \in [0, B]$ with B being an upper bound of x . Note that updating $d^{(k)}$ can constantly change

$D_{D_i}^{(k)}$, $C_{P_i}^{(k)}$, and $C_I^{(k)}$ in (8).

Algorithm 1 The domain-adaptive training strategy of optimizing for da-PINN

-Inputs: (t, x) .
-Initialize: Randomly initialize $\theta_i^{(0)}$ for Net_i and parameters $\lambda^{(0)}$; ($k = 0$).
while the stop criterion is not satisfied **do**
 1) Based on the parameter of interface location $d^{(k)}$, divide training datasets D_D into $D_{D_i}^{(k)}$ and randomly sample collocation point sets $C_{P_i}^{(k)}$ and $C_I^{(k)}$.
 2) Update $\theta_i^{(k)}$ and $\lambda^{(k)}$ according to $Loss^{(k)}$.

$$\begin{cases} \theta_i^{(k+1)} = \theta_i^{(k)} - \eta \nabla_{\theta_i} Loss^{(k)} \\ \lambda^{(k+1)} = \lambda^{(k)} - \eta \nabla_{\lambda} Loss^{(k)} \end{cases}$$

 3) $k = k + 1$.
end while
-Return: The output $\hat{u}_i(t, x; \hat{\theta}_i)$ and $\hat{\lambda}$.

III. EXPERIMENTS

In this section, da-PINN is verified with the one- and two-dimensional Maxwell's equations in heterogeneous media and unknown interface location. All experiments are implemented by Pytorch. Adam is used as the optimizer. The following l_2 relative error is used to evaluate the performance of da-PINN:

$$l_2 \text{ relative error} = \frac{\|\mathbf{u} - \hat{\mathbf{u}}\|_2}{\|\mathbf{u}\|_2},$$

where \mathbf{u} denotes the ground truth and $\hat{\mathbf{u}}$ denotes the corresponding prediction or estimation.

A. One-dimensional Maxwell's Equations

The one-dimensional Maxwell's equations in heterogeneous media under study are as follows:

$$\frac{\partial E_Y}{\partial x} = -\mu \frac{\partial H_Z}{\partial t}, \quad \frac{\partial H_Z}{\partial x} = -\varepsilon \frac{\partial E_Y}{\partial t}, \quad x \in [0, 20], t \in [0, 10]. \quad (9)$$

$\Omega_1 = [0, 10]$ and $\Omega_2 = [10, 20]$ are obtained with $x = 10$ as d . $\varepsilon = 1$ in the whole Ω . To present heterogeneous media, μ is assumed to be a piecewise constant. Here, $\mu_1 = 1$ in Ω_1 and $\mu_2 = 9$ in Ω_2 . The analytical solutions to (9) are as follows:

$$E_Y = \begin{cases} \cos(0.1t - 0.1x + 1) + 0.5\cos(0.1t - 0.1x - 1), & \text{if } x \in \Omega_1 \\ 1.5\cos(0.1t - 0.3x + 3), & \text{if } x \in \Omega_2 \end{cases},$$

$$H_Z = \begin{cases} \cos(0.1t - 0.1x + 1) - 0.5\cos(0.1t - 0.1x - 1), & \text{if } x \in \Omega_1 \\ 0.5\cos(0.1t - 0.3x + 3), & \text{if } x \in \Omega_2 \end{cases},$$

The abovementioned setups are used to generate training and testing datasets. Considering the practical operating environment, λ is assumed to be unknown. In this example, we set $N_D = 2000$, $N_{P1} = N_{P2} = 4000$, and $N_I = 2000$. There are

5 hidden layers and 30 neurons per layer in Net_i . ReLU is used as the activation function. Randomly initialize parameters as $\mu_1^{(0)} = 1$, $\varepsilon_1^{(0)} = 1$, $\mu_2^{(0)} = 13$, $\varepsilon_2^{(0)} = 0$, and $d^{(0)} = 15$. Table I shows the estimation performance. The estimations of

TABLE I
ESTIMATION PERFORMANCE OF DA-PINN FOR ONE-DIMENSIONAL MAXWELL'S EQUATIONS.

Parameters	Estimations	l_2 relative error (%)
μ_1	0.9997	0.0309
ε_1	0.9998	0.0165
μ_2	8.9918	0.0907
ε_2	0.9999	0.0132
d	9.9998	0.0017

parameters ε and μ obtained by da-PINN are shown in Fig. 1. The absolute errors $|u - \hat{u}|$ of E_Y and H_Z obtained by da-PINN and PINNs are shown in Fig. 2. The results indicate that da-PINN achieves better performance, especially near the interface. The l_2 relative errors are listed in Table II, in which the best values are in bold font.

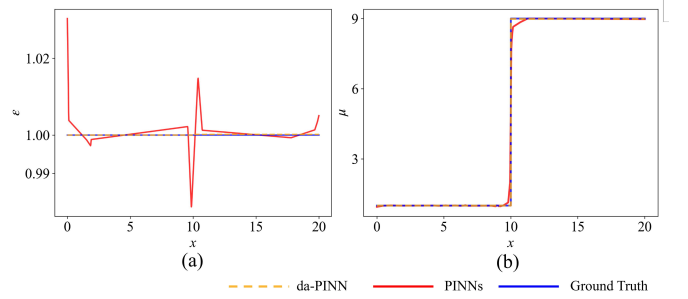


Fig. 1. Estimations obtained by da-PINN and PINNs. (a) Estimations for ε . (b) Estimations for μ .

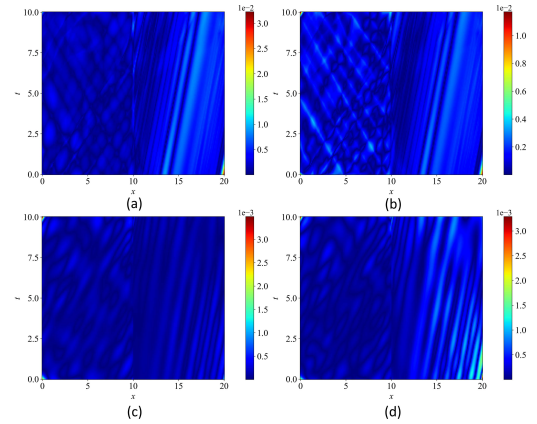


Fig. 2. Absolute errors for predictions to one-dimensional Maxwell's equations. (a) E_Y obtained by da-PINN. (b) H_Z obtained by da-PINN. (c) E_Y obtained by PINNs. (d) H_Z obtained by PINNs.

B. Two-dimensional Maxwell's Equations

The two-dimensional Maxwell's equations under study are as follows:

$$\varepsilon \frac{\partial E_X}{\partial t} = \frac{\partial H_Z}{\partial y}, \quad \frac{\partial E_Y}{\partial x} - \frac{\partial E_X}{\partial y} = -\mu \frac{\partial H_Z}{\partial t}, \quad (10)$$

$$\varepsilon \frac{\partial E_Y}{\partial t} = -\frac{\partial H_Z}{\partial x}, \quad \Omega = x \times y = [0, 2\pi] \times [0, 2\pi], t \in [0, 2].$$

TABLE II
PREDICTION PERFORMANCE OF DA-PINN AND PINNS FOR ONE-DIMENSIONAL MAXWELL'S EQUATIONS.

Methods	Predictions	l_2 relative error
da-PINN	\widehat{E}_Y	6.485e-4
	\widehat{H}_Z	1.120e-3
PINNs	\widehat{E}_Y	2.664e-3
	\widehat{H}_Z	3.627e-3

The analytical solutions to (10) are obtained according to [27]:

$$\begin{aligned} E_X &= \frac{k_Y}{\varepsilon\sqrt{\mu\omega}} \cos(\omega t) \cos(k_X x) \sin(k_Y y), \\ E_Y &= -\frac{k_X}{\varepsilon\sqrt{\mu\omega}} \cos(\omega t) \sin(k_X x) \cos(k_Y y), \\ H_Z &= \frac{1}{\sqrt{\mu}} \sin(\omega t) \cos(k_X x) \cos(k_Y y), \end{aligned} \quad (11)$$

where $\omega = \frac{k_X^2 + k_Y^2}{\mu\varepsilon}$. $\Omega_1 = [0, \pi] \times [0, 2\pi]$ and $\Omega_2 = [\pi, 2\pi] \times [0, 2\pi]$ are obtained with $d = \pi$ as the interface location. The parameters in (11) are as follows:

$$\varepsilon(\mathbf{x}) = \begin{cases} 2, & \text{if } \mathbf{x} \in \Omega_1 \\ 5, & \text{if } \mathbf{x} \in \Omega_2 \end{cases}, \quad k_X(\mathbf{x}) = \begin{cases} 2, & \text{if } \mathbf{x} \in \Omega_1 \\ 4, & \text{if } \mathbf{x} \in \Omega_2 \end{cases},$$

$\mu = 1$, $k_Y = 2$, and $\mathbf{x} = [x, y]$. In this example, we set $N_D = 8000$, $N_{P1} = N_{P2} = 10000$, and $N_I = 5000$. There are 8 hidden layers and 50 neurons per layer in Net_i . We have tried ReLU and tanh as activation functions, in which ReLU with a better result is selected in this letter. $\lambda^{(0)}$ are randomly set as $\mu_1^{(0)} = 2$, $\varepsilon_1^{(0)} = 1$, $\mu_2^{(0)} = 13$, $\varepsilon_2^{(0)} = 0$, and $d^{(0)} = 15$. Table III shows the estimation performance. Fig. 3 shows the comparison of da-PINN and PINNs, in which the estimations of da-PINN are more accurate near the interface. Fig. 4 shows the absolute errors of E_X , E_Y , and H_Z obtained by da-PINN and PINNs, which indicates the relatively large prediction error of E_X obtained by PINNs primarily happens near the interface. The l_2 relative errors of predictions are listed in Table IV. The better values are in the bold font shown in Table IV.

TABLE III
ESTIMATION PERFORMANCE OF DA-PINN FOR TWO-DIMENSIONAL MAXWELL'S EQUATIONS.

Parameters	Estimations	l_2 relative error (%)
μ_1	0.9997	0.0287
ε_1	2.0010	0.0501
μ_2	1.0002	0.0236
ε_2	4.9987	0.0270
d	3.1425	0.0274

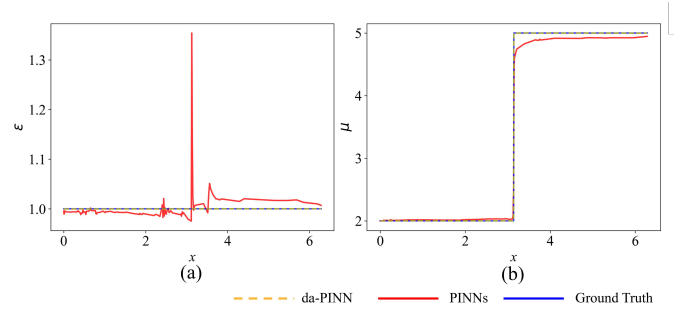


Fig. 3. Estimations obtained by da-PINN and PINNs. (a) Estimations for ε . (b) Estimations for μ .

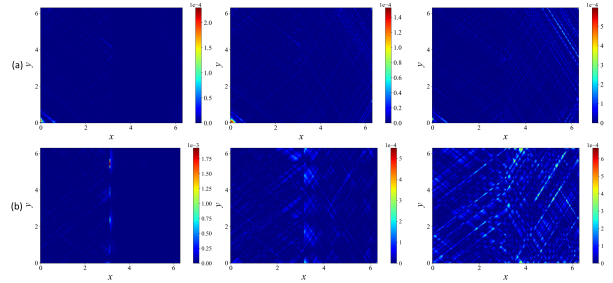


Fig. 4. Absolute errors for predictions. (a) E_X , E_Y , and H_Z obtained by da-PINN. (b) E_X , E_Y , and H_Z obtained by PINNs.

TABLE IV
PREDICTION PERFORMANCE OF DA-PINN AND PINNS FOR TWO-DIMENSIONAL MAXWELL'S EQUATIONS.

Methods	Predictions	l_2 relative error
da-PINN	\widehat{E}_X	7.326e-3
	\widehat{E}_Y	8.189e-3
	\widehat{H}_Z	9.990e-3
PINNs	\widehat{E}_X	1.870e-2
	\widehat{E}_Y	1.239e-2
	\widehat{H}_Z	9.605e-3

IV. CONCLUSIONS

In this letter, we proposed a da-PINN for solving the inverse problems of the Maxwell's equations in heterogeneous media and unknown interface location. In da-PINN, two sub-networks are used to approximate the electric and magnetic fields of sub-domains. The parameters of the Maxwell's equations and interface location are incorporated into the loss function. We also propose a domain-adaptive strategy to train da-PINN. Experimental results verify the effectiveness of our method.

In the future, we will extend da-PINN to solve the Maxwell's equations in heterogeneous media with unknown shapes of interface. This will enable da-PINN to solve more complex problems of the Maxwell's equations.

REFERENCES

- [1] A. Ebrahimijahan, M. Dehghan, and M. Abbaszadeh, "Simulation of maxwell equation based on an adi approach and integrated radial basis

- function-generalized moving least squares (irbf-gmls) method with reduced order algorithm based on proper orthogonal decomposition,” *Engineering Analysis with Boundary Elements*, vol. 143, pp. 397–417, 2022. [Online]. Available: <https://www.sciencedirect.com/science/article/pii/S095579972200217X>
- [2] Z. Xiao and J. He, “Modeling of metallic landmine electromagnetic characteristic in gpsar,” in *2008 International Conference on Microwave and Millimeter Wave Technology*, vol. 4, 2008, pp. 1896–1898.
 - [3] X. Lin, Y. Ding, Z. Gong, and Y. Chen, “Hybrid microwave medical imaging approach combining quantitative and qualitative algorithms,” *IEEE Antennas and Wireless Propagation Letters*, vol. 20, no. 4, pp. 438–442, 2021.
 - [4] J. Wang, Z. Zhao, J. Wu, K. Yang, Z. Nie, and Q.-H. Liu, “Electromagnetic inverse scattering series (iss) method for sensing 2-d objects buried in layered media with unknown dielectric properties,” in *2013 IEEE Antennas and Propagation Society International Symposium (APSURSI)*, 2013, pp. 536–537.
 - [5] S. Pandit, A. Mohan, and P. Ray, “Low-rcs low-profile four-element mimo antenna using polarization conversion metasurface,” *IEEE Antennas and Wireless Propagation Letters*, vol. 19, no. 12, pp. 2102–2106, 2020.
 - [6] Y. Chen, M. Zhong, Z. Guan, and F. Han, “A tailored semiphysics-driven artificial neural network for electromagnetic full-wave inversion,” *IEEE Transactions on Antennas and Propagation*, vol. 70, no. 8, pp. 6207–6217, 2022.
 - [7] S. Zhao and G. Wei, “High-order ftdt methods via derivative matching for maxwell’s equations with material interfaces,” *Journal of Computational Physics*, vol. 200, no. 1, pp. 60–103, 2004. [Online]. Available: <https://www.sciencedirect.com/science/article/pii/S0021999104001330>
 - [8] P. Monk, “Analysis of a finite element method for maxwell’s equations,” *SIAM Journal on Numerical Analysis*, vol. 29, no. 3, pp. 714–729, 1992. [Online]. Available: <https://doi.org/10.1137/0729045>
 - [9] M. Moghaddam and W. C. Chew, “Study of some practical issues in inversion with the born iterative method using time-domain data,” *IEEE Transactions on Antennas & Propagation*, vol. 41, no. 2, pp. 177–184, 1993.
 - [10] Z. Nie and F. Yang, “Variational born iteration method and its applications to hybrid inversion,” *IEEE Transactions on Geoscience & Remote Sensing*, vol. 38, no. 4, pp. 1709–1715, 2000.
 - [11] J. Li, H.-J. Hu, J. Wang, M. Zhuang, L.-Y. Xiao, and Q. H. Liu, “A transceiver-configuration-independent 2-d electromagnetic full-wave inversion scheme based on end-to-end artificial neural networks,” *IEEE Transactions on Antennas and Propagation*, vol. 71, no. 5, pp. 4600–4605, 2023.
 - [12] F. Wu, M. Fan, W. Liu, B. Liang, and Y. Zhou, “An efficient time-domain electromagnetic algorithm based on lstm neural network,” *IEEE Antennas and Wireless Propagation Letters*, vol. 20, no. 7, pp. 1322–1326, 2021.
 - [13] R. Molinaro, Y. Yang, B. Engquist, and S. Mishra, “Neural inverse operators for solving pde inverse problems,” *arXiv preprint arXiv:2301.11167*, 2023.
 - [14] R. Maziar, P. Paris, and K. G. Em, “Physics informed deep learning (part ii): Data-driven discovery of nonlinear partial differential equations,” *arXiv preprint arXiv: 1711.10566*, 2017.
 - [15] A. D. Jagtap, Z. Mao, N. Adams, and G. E. Karniadakis, “Physics-informed neural networks for inverse problems in supersonic flows,” *Journal of Computational Physics*, vol. 466, p. 111402, 2022. [Online]. Available: <https://www.sciencedirect.com/science/article/pii/S0021999122004648>
 - [16] T. Kapoor, H. Wang, A. Nunez, and R. Dollevoet, “Physics-informed neural networks for solving forward and inverse problems in complex beam systems,” *arXiv preprint arXiv:2303.01055*, 2023.
 - [17] Y. Chen, L. Lu, G. Karniadakis, and L. Negro, “Physics-informed neural networks for inverse problems in nano-optics and metamaterials,” *Optics Express*, vol. 28, 03 2020.
 - [18] Y. Ye, H. Fan, Y. Li, X. Liu, and H. Zhang, “Deep neural network methods for solving forward and inverse problems of time fractional diffusion equations with conformable derivative,” *Neurocomputing*, vol. 509, pp. 177–192, 2022.
 - [19] T. Kapoor, H. Wang, A. Núñez, and R. Dollevoet, “Physics-informed machine learning for moving load problems,” *arXiv preprint arXiv:2304.00369*, 2023.
 - [20] Y. Li, T. Theodoulidis, and G. Y. Tian, “Magnetic field-based eddy-current modeling for multilayered specimens,” *IEEE Transactions on Magnetics*, vol. 43, no. 11, pp. 4010–4015, 2007.
 - [21] V. Chernyshov, A. Kaz’min, and P. Fedyunin, “Testing electrophysical parameters of multilayer dielectric and magnetodielectric coatings by the method of surface electromagnetic waves,” in *2021 3rd International Conference on Control Systems, Mathematical Modeling, Automation and Energy Efficiency (SUMMA)*, 2021, pp. 372–377.
 - [22] S. A. Faroughi, N. Pawar, C. Fernandes, S. Das, N. K. Kalantari, and S. K. Mahjour, “Physics-guided, physics-informed, and physics-encoded neural networks in scientific computing,” *arXiv preprint arXiv:2211.07377*, 2022.
 - [23] Y. Chen and L. Dal Negro, “Physics-informed neural networks for imaging and parameter retrieval of photonic nanostructures from near-field data,” *APL Photonics*, vol. 7, no. 1, 2022.
 - [24] Y. Zhang, H. Fu, Y. Qin, K. Wang, and J. Ma, “Physics-informed deep neural network for inhomogeneous magnetized plasma parameter inversion,” *IEEE Antennas and Wireless Propagation Letters*, vol. 21, no. 4, pp. 828–832, 2022.
 - [25] A. G. Baydin, B. A. Pearlmutter, A. A. Radul, and J. M. Siskind, “Automatic differentiation in machine learning: a survey,” *Journal of Machine Learning Research*, vol. 18, pp. 1–43, 2018.
 - [26] Cheng and DavidK, *Field and wave electromagnetics /-2nd ed.* Field and wave electromagnetics /-2nd ed, 2007.
 - [27] C. Niu and H. Ma, “A high-order accurate multidomain legendre–chebyshev spectral method for 2d maxwell’s equations in inhomogeneous media with discontinuous waves,” *Applied Mathematics Letters*, vol. 128, p. 107906, 2022. [Online]. Available: <https://www.sciencedirect.com/science/article/pii/S0893965922000027>